

Optical Properties of OPEs

Subjects: Chemistry, Organic

Contributor: Anna Barattucci

Oligophenylene ethynyls, known as OPEs, are a sequence of aromatic rings linked by triple bonds, the properties of which can be modulated by varying the length of the rigid main chain or/and the nature and position of the substituents on the aromatic units. They are luminescent molecules with high quantum yields and can be designed to enter a cell and act as antimicrobial and antiviral compounds, as biocompatible fluorescent probes directed towards target organelles in living cells, as labelling agents, as selective sensors for the detection of fibrillar and prefibrillar amyloid in the proteic field and in a fluorescence turn-on system for the detection of saccharides, as photosensitizers in photodynamic therapy (due to their capacity to highly induce toxicity after light activation), and as drug delivery systems.

Keywords: oligophenylene ethynyls ; luminescent probe

1. Background

The idea of using aryl and ethynyl groups in an alternating fashion to build polymers such as polyphenylene ethynyls (PPEs) and their corresponding oligomers (OPEs) was introduced in the 1980s, and this led to the discovery of a class of compounds with fascinating properties as materials in different areas, such as sensors, light-emitting devices, and polarizers for LC displays. The polymeric PPEs consist of mixtures of molecules with a broad size range and with no perfect control of sequences; moreover, PPEs tend to form aggregates easily through intra- and/or interchain stacking, in turn reducing their solubility and thus their application in an aqueous environment ^[1].

For the mentioned reasons, in the last decades the attention of the scientific community has been focused mainly on oligophenylene ethynyls (OPEs) and their peculiar characteristics and applications in the biological field. The rigid control of the chain lengths in OPEs implies well-defined chemical and physical properties (e.g., solubility), thus allowing for precise interpretations of their actions in biology and definite applications in medical fields.

OPEs can be designed with a controlled monomer sequence, which represents a key feature for their application in biological processes, where the activity of a cell is dramatically influenced by very small environmental and structural changes. Due to their stable π -conjugated rigid skeleton, OPEs are luminescent dyes, with high quantum yields. The presence of aromatic rings linked by triple bonds guarantees a high electron conjugation and, consequently, a prominent absorption of λ_{max} at ~ 400 nm, which can be tuned by varying the number of aromatic units and/or the substituents. In particular, a larger number of aromatic rings and the presence of donor substituents usually lead to bathochromic shifts, while the presence of acceptor groups seems to be less effective in changing the absorption properties of OPEs. Their emission properties can be modulated by modification of the structure. In the interaction with an analyte or with target molecules, even little changes in the structure (length or monomer compositions) can deeply influence the spectral outputs, allowing us to use them as sensors or as probes. They can be easily differently functionalized by inserting various side chains and/or end groups and numbers of repeating units; this offers us useful spectral information due to several interaction mechanisms with the target (e.g., columbic and/or hydrophobic interactions, solvent quenching effects, and variation of rotational freedom in the backbone). The linear repetitive chain of phenylene ethynyls is usually decorated at the two extremities (these OPEs are usually called end-only OPEs) or at the core of symmetric ones (these OPEs are sometimes called S-OPEs). Some of them possess a core different from a benzene ring, such as a thienyl moiety (these compounds are sometimes called oligoarylene ethynyls, OAEs). Unsymmetrically substituted OPEs bear two different substituents attached at the two ends of the main oligomeric chain.

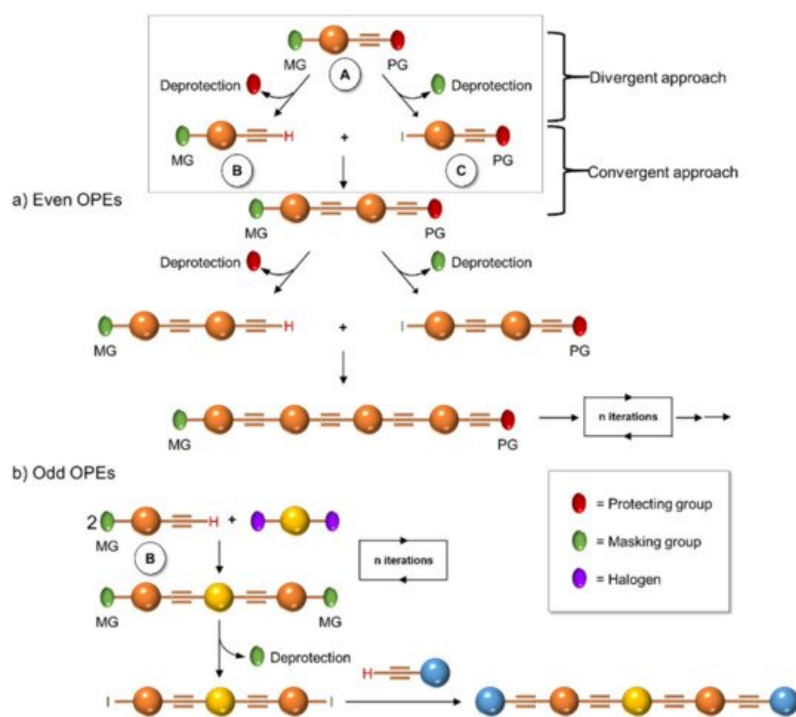
2. Synthesis of OPEs

The first synthetic procedure for the polymerization of the aryl-ethynyl moiety was described by Lakmikantham et al. in 1983 ^[2] and was performed via a cuprous acetylide. From that time, more convenient methodologies have been applied, and almost all of them are based on the palladium-catalyzed, cross-coupling reaction of Heck–Cassar–Sonogashira (referred to as Sonogashira reaction or coupling from now on). In a review on the synthesis, properties, structure, and

applications of PPE—a work that represents a landmark for many researchers who approached the synthesis of PPEs and OPEs—Bunz [1] gave a detailed and critical discussion on the conditions of such reaction, with respect to the Pd catalyst, the aryl halogen, and the alkynyl derivatives, the base, and the solvent.

In general, sequence-defined oligomers, such as OPEs, can be synthesized by iterative processes in which the coupling of protected monomers, followed by deprotection, are steps that are repeated cyclically until the desired oligomer is obtained. Three main approaches to this general process have been investigated in literature: the solution synthesis, the soluble support-based synthesis, and the solid-phase synthesis [2]. Although the last two methodologies appear the most convenient ones, in terms of purification steps and final yields, classical solution chemistry is the most applied and the one we discuss in this section.

In 1994, Tour et al. [4] presented an iterative divergent/convergent approach to the synthesis of OPEs that has been applied afterwards to the preparation of such molecular wires by several other authors [5][6]. The procedure implies, as a fundamental step, the synthesis of a monomer, such as **A** (Scheme 1), consisting of a protected ethynyl group (PG) linked to an aryl moiety, which in turn possesses in *para* position a masking group of iodide (MG). Each of these protecting groups was removed alternatively in the presence of the other, and the two new monomers **B** and **C** were coupled with each other, doubling the length of the molecule. Successive selective deprotections that were followed by dimerization allowed for the access to oligomers with an even number of phenylene ethynylene moieties (Scheme 1a). The same synthetic approach was used by Moggio et al. [7][8] for the preparation of three families of odd side-chain-substituted OPEs (Scheme 1b), two of which were studied as mesomorphic materials. Compound **1** in Table 1, belonging to the most recent family of R-terminated (dodecyl)benzoateethynylene oligomers, was applied in the staining of bacteria [9].



Scheme 1. Schematic representation of iterative divergent/convergent synthetic approaches for even (a) and odd (b) OPEs.

Table 1. Reported OPEs and their bibliographic references.

Entry	Structure	Bibliographic References
1		[9]
2		[5][6]
3		[10]

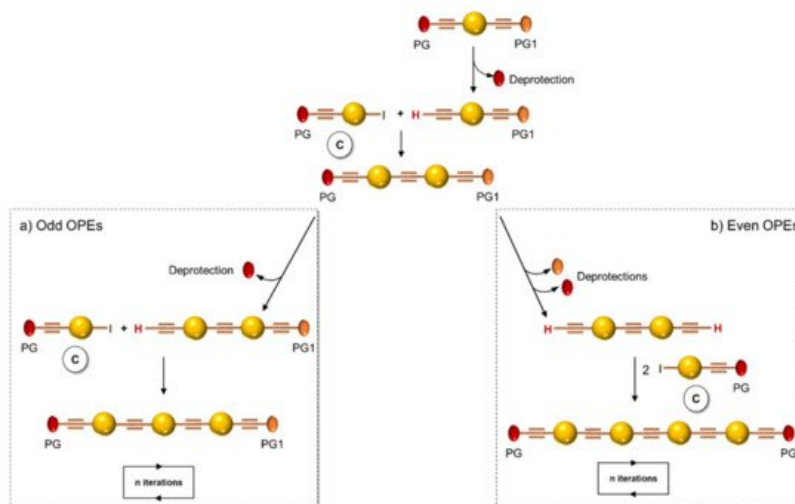
Entry Structure

Bibliographic References

16			[18]
17			[19]
18			<p>$n=1$ 18a</p> <p>$R'=H$ $n=2$ 18b</p> <p>$n=3$ 18c [20][21][22][23][24][25]</p> <p>$n=1$ 18d [26][27][28][29][30][31]</p> <p>$R'=COOEt$ $n=2$ 18e</p> <p>$n=3$ 18f</p>
19			<p>$R'=H$ 19a</p> <p>$R'=COOH$ 19b [20][21][22][23][24][31]</p> <p>$R'=COOEt$ 19c [32]</p>
20			[33]
21			[33]
22	<p>$n = 2, 3, 4, 5, 6, 7, 8, 9$</p>		[34][35]
23			<p>$n=2$ 23a</p> <p>$n=3$ 23b</p> <p>23c [36][26][27][28][29][30]</p> <p>[37][38][39][40][31][32]</p> <p>23d</p> <p>$R = [O(CH2)3N+(CH3)2] Br-$</p>
24		<p>$R=H$</p> <p>$R=COOEt$</p>	<p>$n=1$ $m=2$ 24a</p> <p>$n=2$ $m=2$ 24b</p> <p>$n=1$ $m=3$ 24c [41][25][38][40][31]</p> <p>$n=2$ $m=3$ 24d</p> <p>$n=3$ $m=3$ 24f</p>
25		<p>$R=H$</p> <p>$R=O(CH2)2NH2$</p>	<p>$n=2$ 25a</p> <p>$n=3$ 25b [42][41]</p> <p>$n=3$ 25c</p>

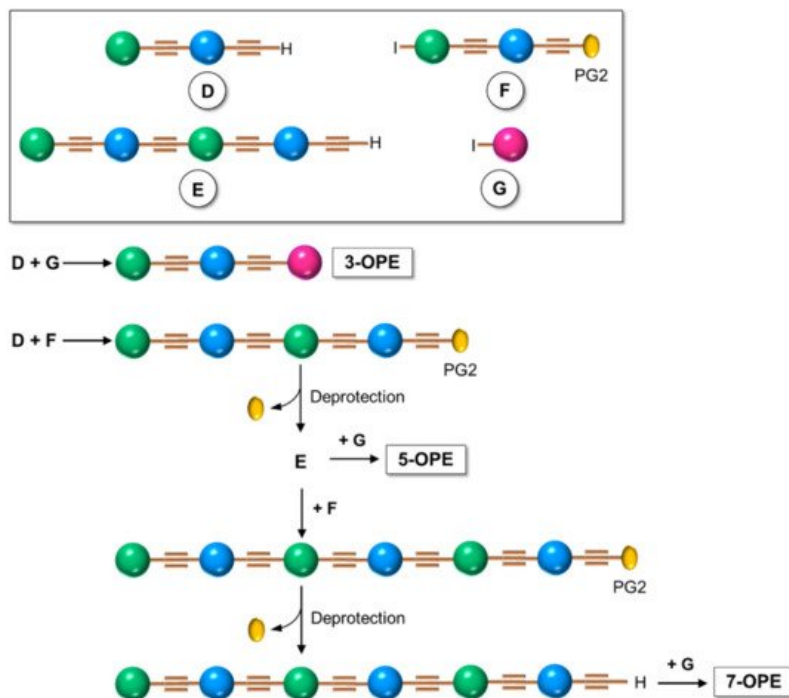
Entry	Structure	Bibliographic References	
26		[42]	
27		n=2 27a n=3 27b	[42][43]
28		R = $\text{---}(\text{CH}_2)_n\text{N}(\text{CH}_3)_3^+$ n=2 28a n=3 28b	[37][44][38][40]
29		R =	28c
29		R = $\text{---}(\text{CH}_2)_3\text{N}(\text{CH}_3)_3^+$	

Inspired by the iterative divergent/convergent approach, Pertici et al. [5] used as the starting brick of their syntheses a *para*-substituted bis-ethynylbenzene possessing two different protecting groups (PG and PG1) of the triple bond (Scheme 2). In playing on the different degrees of lability of the protecting groups for selective removal and doubling the Sonogashira reactions with the opportunely substituted monomer **C**, the authors afforded symmetrical even and odd OPEs with terminal triple bonds. The obtained oligomers were converted by the copper(I)-catalyzed azide–alkyne cycloaddition (CuAAC) into pseudo-disaccharides. In particular, **2** (Table 1) was used for the inhibition of lectin A from *Pseudomonas aeruginosa* (*P. aeruginosa*) [5][6].

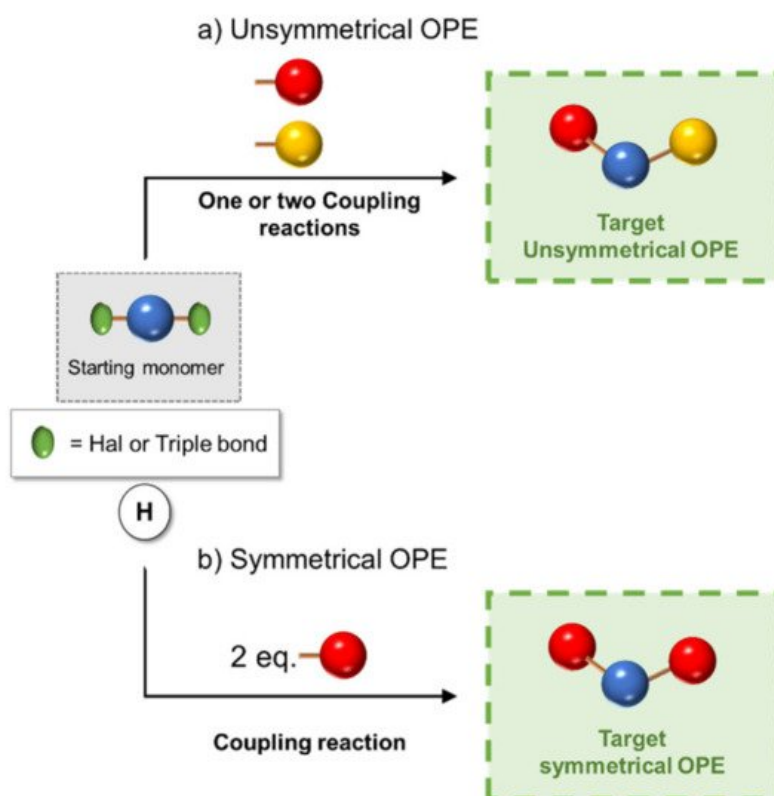


Scheme 2. Schematic representation of iterative divergent/convergent synthetic approach by Pertici et al. [5].

Although the iterative divergent/convergent approach appears effective in the synthesis of OPEs, not all of them can be obtained by this route. The step-by-step solution synthesis of the OPE skeleton, conducted by a series of Sonogashira cross-couplings, in which an opportunely substituted arylalkyne was attached to a conveniently substituted iodobenzene, allowed for the building up of a series of symmetrical and unsymmetrical oligomers with a more original weaving. In particular, unsymmetrical oligomers, where two different substituents are attached at the two ends of the main chain, are the most difficult to be reached: several different building blocks must be prepared and connected to each other (Scheme 3) in a series of frequently low-yielding steps, and the more blocks there are, the longer the OPE's skeleton is. This is what Whitten et al. [45] described in their last review. Unsymmetrical OPEs containing $-(\text{PhC}\equiv\text{C})_n-$ chains have been prepared through Sonogashira-coupling of *para*-substituted aryleneethynylenes (such as **H** in Scheme 4) with 1-iodo-4-(trimethylsilylethynyl)benzene (such as **C** in Scheme 1), followed by the desilylation and iteration of the coupling, until the desired number of phenylethynylene units was obtained [14].



Scheme 3. Schematic representation of the step-by-step synthetic approach for unsymmetrical OPEs.



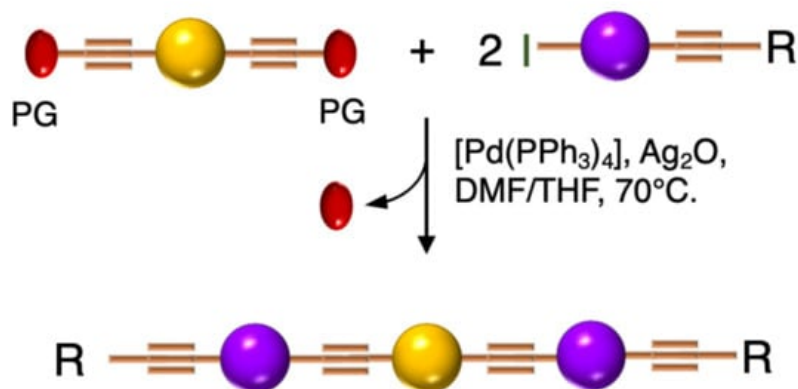
Scheme 4. Schematic representation of (a) unsymmetrical and (b) symmetrical 3-OPEs synthetic approach.

However, if the oligomer consists of just three repetitive arylethynylene units (3-OPE), the synthesis is concerned with the preparation of a central core, which can be made, for example, of an aryl ring bifunctionalized in *para* position with two halogen atoms (iodine or bromine), and of two *para*-substituted arylethynylene moieties, different from each other (Scheme 4a). The three building blocks are finally subjected to the Sonogashira cross-coupling reaction, as shown in Scheme 4a [10][42].

Only two building blocks are necessary for the synthesis of symmetrical (identical ends of the oligomer) 3-OPEs: a bifunctionalized aryl core connected with 2 equivalents of a side-armed aryl derivative, both opportunely substituted (Scheme 4b) [41][11].

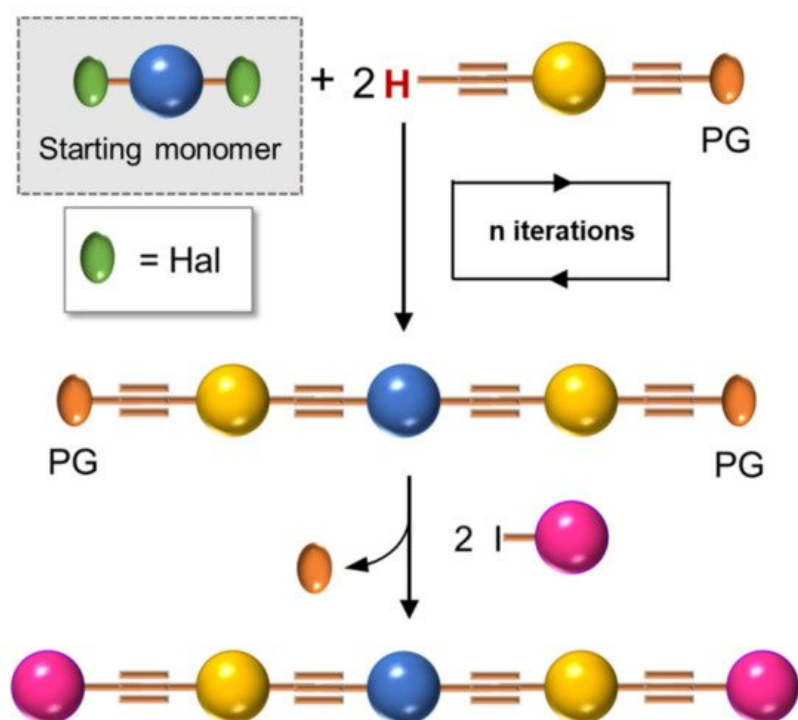
The symmetrical 3-OPE **3** (Table 1), bearing two 4-aminophenyl- β -D-mannopyranoside end-moieties, was synthesized with the same general approach described in Scheme 4b and used as specific fluorescent marker as well as transducer for the detection of *Escherichia coli* (*E. coli*) [10].

Barattucci et al. [11][12][13] reported the synthesis of a series of 3-OPEs (**5–10** in Table 1) in which the substituents at the aryl cores are different from those on the aryl moieties of the two side arms, and they also described how such substituents influence the bioaffinity of oligomers under study. The introduction of a NMe₂ group and its subsequent quaternarization, for instance, led to the preparation of biocompatible probes **7** and **10** [13]. The Sonogashira reaction conditions adopted by these authors consider the use of a trimethylsilyl (TMS)-protected arylethynylene derivative and an aryl iodide, in the presence of a palladium catalyst and silver oxide, as the base, thus avoiding the tedious step of the triple bond deprotection (Scheme 5) [11][12][46].



Scheme 5. Schematic representation of 3-OPEs synthetic approach via Ag₂O-based Sonogashira coupling.

Finally, most of the preparation of symmetrical oligomers longer than 3-OPEs involves the use of several synthetic steps, as shown in Scheme 6, where the iteration of protection/deprotection steps and Sonogashira reactions represents, once again, the basis of the synthesis [45].



Scheme 6. Schematic representation for preparation of symmetrical OPEs longer than three repetitive units.

3. Optical Properties of OPEs

In fluorescence bioimaging, after excitation, a molecular probe produces luminescence in the visible or in the near-infrared region of the spectrum; the signal is then collected and elaborated through detection equipment that provides an image of the biological tissues. It represents an important visualizing technique and possesses many advantages in comparison with others, such as radiolabeling or magnetic resonance imaging (MRI), because of its high sensitivity, good spatial/temporal resolution, and low damages done to tissues. Furthermore, the fluorescent probe can be labeled with

targeting moieties in order to direct its absorption in definite biological compartments. Depending on the physiological environment, the probe can change its photophysical properties, can be activated [47], and thus be used for biosensing. In the last decades, many elegant fluorescent sensing mechanisms have been developed, and many luminescent systems have been used for fluorescence bioimaging in vitro and/or in vivo [48]: inorganic nanomaterials [49], supramolecular assemblies [50], and organic fluorophores [51]. Among them, organic dyes are widely used as imaging and sensing agents (ISAs) in optical microscopy. Due to their interesting fluorescence features, one of the more intuitive uses of OPEs is their application as an ISA in the biological field, after having overcome any problems of water solubility and cytotoxicity. This section comprises two main subjects: OPEs as probes for targeted imaging and theragnostics and OPEs in the field of biosensing.

3.1. OPEs as Probes

A series of differently functionalized OPEs were derivatized with a lysine-reactive N-hydroxysuccinimidyl (NHS) group in order for them to be able to covalently attach to proteins, such as HSA (human serum albumin) acting as highly fluorescent labels [14]. In the study, the authors synthesized and characterized a series of OPEs (**11**, Table 1) bearing different functional groups. Among them, **11b** was subjected to cytotoxicity studies on lung cancer cells, and it showed very good IC₅₀ values, thus confirming the good biocompatibility of this class of molecules. HSA, the model protein, was labeled with compounds **11a–f**; the OPE-HSA conjugates were investigated by MALDI-TOF mass spectrometry and UV-Vis absorption spectroscopy, and they showed a degree of labeling varying from 10 to 3, with good accordance of results between the two techniques. Interestingly, OPE luminescence, which is very low in aqueous media (DMF/H₂O and DMF/PBS), dramatically increased after protein conjugation; the labeling was also studied using sodium dodecyl sulfate polyacrylamide gel electrophoresis (SDS-PAGE). When irradiated under UV light, the OPE-HSA conjugates exhibit a green fluorescence, which is correlated to their emission quantum yields. Furthermore, through PAGE studies, no changes in the mobility of HSA were found after functionalization with fluorescent probes. These stimulating results paved the way to use OPEs as label agents also for other biomolecules.

In 2014 Huang et al. [15] reported the amphiphilic OPE **12** in Table 1, bearing hydrophobic alkyl and methoxy-polyethyleneglycol (MPEG) hydrophilic chains. It can be obtained via Sonogashira coupling (Scheme 4, unsymmetrical) and is able to self-assemble into nanoparticles (Figure 1) with good water solubility, good stability, and excellent spectroscopic features, useful for cellular imaging through confocal laser scanning microscopy (CLSM) imaging. By varying the lengths of the MPEG pendants (OPE-PEG₃₅₀, OPE-PEG₅₀₀, OPE-PEG₁₀₀₀, OPE-PEG₁₉₀₀), it was possible to modulate the solubility, morphology, and size of the nanoparticles. The spectroscopic features of all OPE-PEGylated derivatives in THF consist of a strong absorption peak at 330 nm and an emission peak at 425 nm, due to a single OPE molecule. Meanwhile, in water the absorption and fluorescence spectra of OPE-PEG₁₉₀₀ **12** (10⁻⁵ mol L⁻¹) suggested the formation of H- and J-aggregates at lower and higher concentrations, respectively, as confirmed by fluorescence lifetime studies. In order to evaluate their applicability for in vivo imaging, the stability of the nanoparticles was tested in calf serum (CS), and no precipitation was observed after centrifugation, even three months later. The photostability was also tested, and after 20 min of UV irradiation, the nanoparticles showed a good stability, probably due to the shielding of the aromatic core from oxygen by MPEG. The cytotoxicity, evaluated in human pancreatic cancer cells (PANC-1) by an MTT cell viability assay, revealed their high biocompatibility, mainly for OPE-PEG₁₉₀₀ **12**. A CLSM visualization in vitro, performed after 18 h of incubation, showed a blue fluorescence (410–470 nm) located in the cytoplasm, thus indicating OPE-PEG₁₉₀₀ **12** as a good and stable bioimaging cell system.

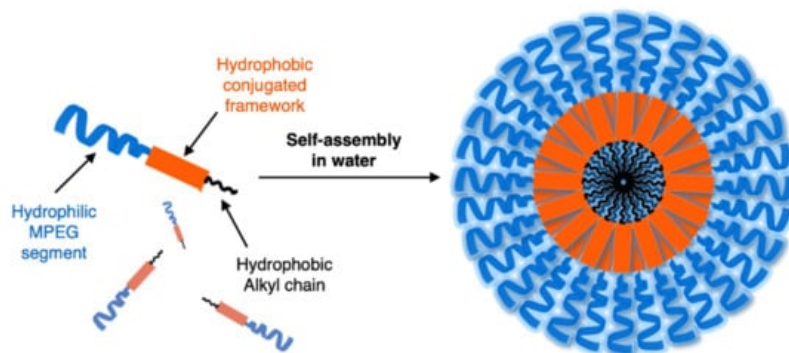


Figure 1. Schematic representation of amphiphilic OPE and its self-assembly into nanoparticles in water.

Huang et al. [16] developed fluorescent water-soluble diamino polyethylene glycol (PEG-NH₂) OPEs **13** (Table 1), corroborating the ability of such OPE derivatives to self-assemble into nanoparticles with different morphologies, by simply adjusting the concentrations in aqueous solution. The spectroscopic studies of the nanoparticles in water suggested

typical J-aggregate behavior. The fluorescence micrograph showed vivid blue emitting nanoparticles well dispersed in water solution, and TEM images showed different morphologies, i.e., grain-like structures at lower concentrations and strawberry-like structures at higher concentrations. The biocompatibility of such OPE-based nanoparticles was tested by an MTT assay on PANC-1 cells, and good cell viability was observed (>90%). Furthermore, live cells imaging after the incubation of OPE **13** was performed by CLSM, and a strong fluorescence at 720 nm was recorded in the cellular cytoplasm, thus providing a long-term and spatially resolved imaging with reduced cell damages. Starting from these interesting results, Huang's group [17] developed fluorescent magnetic nanoparticles (FMNPs), using iron oxide nanocrystals decorated by amphiphilic PEG-functionalized OPEs. Amino-modified PEG pendants were introduced as a hydrophilic portion (MNPs@OPE-PEG-NH₂ **14a**, Table 1) and a folate as targeting moiety (MNPs@OPE-PEG-FA **14b**, Table 1). The folate was introduced in the OPE because its receptor is highly expressed on the cell surface of many kind of cancer cells. Such FMNPs were characterized by UV-Vis absorption and photoluminescence spectroscopy, confirming the formation of H-type assemblies on the surface of MNPs. The magnetic resonance analysis showed a very efficient contrast agent ability of MNPs@OPE. The biocompatibility of such MNPs (**14a** and **14b**) was evaluated by an MTT assay using 3T3 fibroblasts, which showed a good viability of the cell treated with both types of nanoparticles. To investigate the targeting ability of the nanoparticles, HeLa cancer cells were incubated with both MNPs, leading to a significant negative contrast enhancement for the magnetic resonance imaging of MNPs@OPE-PEG-FA **14b**. The specific internalization of the nanoparticles was higher for **14b** in the HeLa cells and in particular in the cytoplasm, while for MNPs@OPE-PEG-NH₂ **14a** a weak fluorescence was recorded in the 3T3 fibroblasts, confirming the targeting ability of folate nanoparticles. The dual imaging ability of MNPs@OPE-PEG-FA **14b** was also tested in vivo, using animal tumor bearing models, and their selective internalization was confirmed by a Prussian blue staining test, with a high quantity of iron in the MNPs@OPE-PEG-FA **14b** treated tissues. Unfortunately, the low emission wavelength (460 nm) prevents their use for fluorescence imaging in vivo, but nevertheless the system can still be used for the optical imaging of tissues in biopsies and thus for postoperative analysis.

Barattucci et al. [11] developed new OPE-glucoside conjugates **5-6** (in Table 1) for cellular uptake and visualization. A series of 3-OPEs that possess acetyl-protected or unprotected β -D-glucopyranose terminations, with differently substituted aromatic cores, were obtained through the general procedure illustrated in Scheme 4. Very significant results were obtained with compound **6a**, where the introduction of a NMe₂ group in the central aromatic core produced an interesting modulation of the emission profile and improved the internalization performed using human larynx epidermoid carcinoma tissue cells (Hep-2). Moreover, compound **6a** was found localized mainly in the cytoplasm, which allowed for visualization through fluorescence microscopy already at 1 μ M of OPE. Furthermore, the protected compound **6c** was slightly internalized in Hep-2 cells. Additionally, the cell viability, tested with trypan blue assay, showed a good biocompatibility of these OPEs, confirming the possibility to use them as modifiable platforms for bioimaging. The presence of one or two positive charges in the dialkylamino-substituted OPEs **7** and **10a** (Table 1) improves water solubility and, in cooperation with "H-bonding" sugar groups, makes them able to interact with DNA [13]. The noncovalent interactions with DNA were characterized by hypochromicity and accompanied by a red and a blue shift for dicationic **10a** and monocationic OPEs **7**, respectively. Circular dichroism studies and the different spectroscopic behaviors have suggested a mixed binding mode of OPEs **7** and **10a** with the biopolymer, ascribable to intercalation (suggested by absorption titrations and melting temperature measurements) and an external interaction (suggested by CD and viscosity results). Thus, it was reported by the authors that the positively charged OPEs **7** and **10a** were first electrostatically attracted by negative DNA backbone and then inserted the aromatic core between DNA bases. At the same time the glucose groups stabilized the interaction through hydrogen bonds. The biocompatibility of OPEs was tested on healthy Vero cells (African green monkey kidney cells) and Hep-2 cancer cells; no toxicity for OPEs was found in the healthy cells, and a reduction of cellular proliferation was seen in the Hep-2 cell for the dicationic OPE **10a**. This result was attributed to a different cellular uptake process with respect to monocationic OPE **7**, joined to the more pronounced mitosis in cancer cells, with the exposure of genetic materials, which supports the higher sensitivity of OPE **10a** to Hep-2 with respect to healthy cells.

An innovative imaging system, one based on orthogonal reactions that take place in a biological environment, was developed by Wang et al. in 2018 [19]. They used modified OPEs **15** and **16** (Table 1) to target mitochondria through "bioorthogonal reactions". Mitochondria are very important organelles that are present in the eukaryotic cells, and they are involved in energy production and in many other biological processes. In OPE **15**, the presence of tetrazine induced a turn-off of the luminescence through bond-energy transfer (TBET). When the tetrazine-substituted OPE **15** reacts, inside the cell, in a "bioorthogonal reaction" with an opportune dienophile synthesized by the authors (MITO-TCO) and containing a tri-phenyl phosphine moiety (TPP), the intra-MITO derivative **16** is obtained and the fluorescence turns on, allowing for the visualization of the cell compartments (Figure 2b). By CLMS measurements, it was possible to confirm a

good overlap between intra-MITO **16** (blue fluorescence) and the dye MITO-tracker (red fluorescence), confirming the good targeting ability of the TPP group, after bioorthogonal intracellular reaction. The realized system was able to be directed towards mitochondria and visualize them, offering a guide also for other kinds of organelles in living cells.

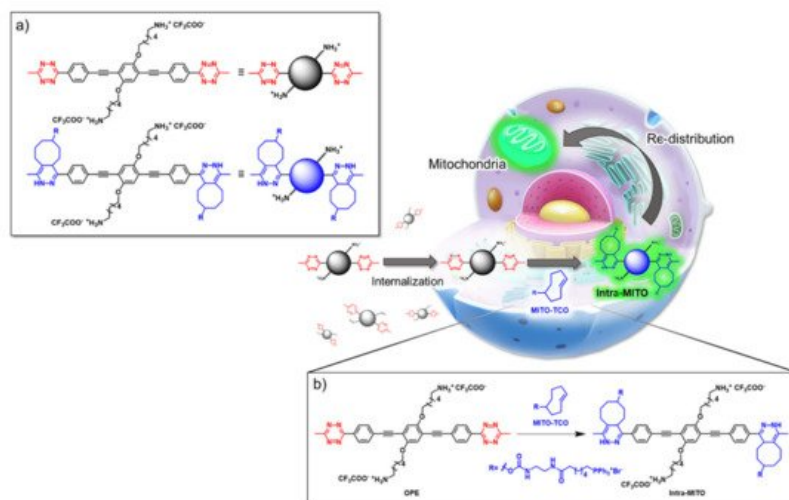


Figure 2. Schematic illustration of the mitochondria-targeting process of tetrazine-conjugated OPE **15** in living cells: (a) the simplified representation of OPEs **15** and **16**; (b) the intracellular synthesis of fluorescent intra-MITO.

The possibility of using OPE derivatives for dual imaging and drug-carrying systems represents a goal for many scientists. In 2019, Maji et al. [19] developed a metal organic hybrid system for imaging and drug delivery that is based on functionalized OPEs possessing solvent-adaptive behavior. These oligomers form a nanoscale metal organic framework (NMOF) with different morphologies, depending on the solvent (Figure 3a). In particular, carboxylic functionalized OPE **17** (Table 1), used as chelating for Zn(II), was decorated with alkyl and glycol chains and was able to form three nontoxic and reversibly shaped NMOFs: nanovesicle (NMOF-1), inverse nanovesicle (NMOF-2), and nanoscroll (NMOF-3). Since the NMOF was assembled through hydrogen bonds and the π - π interaction between PEG and alkyl chains, respectively, the authors tried to change the shape of the nanosystem by varying the solvent polarity. Interestingly, the morphology of the system can be modulated by passing through THF \rightarrow H₂O \rightarrow methanol, in turn obtaining NMOF-1 \rightarrow NMOF-2 \rightarrow NMOF-3, in a reversible fashioned way. In addition, all systems showed an OPE typical cyan emission (43% of quantum yield) and thus were used for living cell bioimaging on HeLa (human cervical cancer) cells. After treating HeLa cells with NMOF-1, a cyan emission in structured illumination microscopy (SR-SIM) was recorded, confirming its efficient uptake. Considering the good ability of internalization of NMOF-1, the nanovesicles were loaded with cisplatin (cisplatin@NMOF-1 loading amount of 14.4 wt%). The loading was monitored by different techniques, which suggests a change in the morphology of a cisplatin-loaded system when passing from NMOF-1 to NMOF-3 shape, with cisplatin homogeneously encapsulated in the nanoscroll (Figure 3b). In vitro release studies showed a release of drugs from 67% up to 82% with a good stability of NMOF. Furthermore, the in vitro studies on HeLa cells incubated with cisplatin@NMOF-1 and with NMOF-1 as control showed a high toxicity ($IC_{50} = 0.5 \mu\text{M}$) for cisplatin@NMOF-1 and no toxic behavior for the control, confirming the good ability of NMOF as a nanocarrier and delivery system. Similar studies were conducted with doxorubicin (DOX), a commercial anticancer drug: in this case, although it had a lower loading capability (4.1 wt%), the release was of 99%. According to these studies, the innovative solvent-adapting nanovesicle system that was developed can represent a very good and versatile drug delivery and bioimaging system.

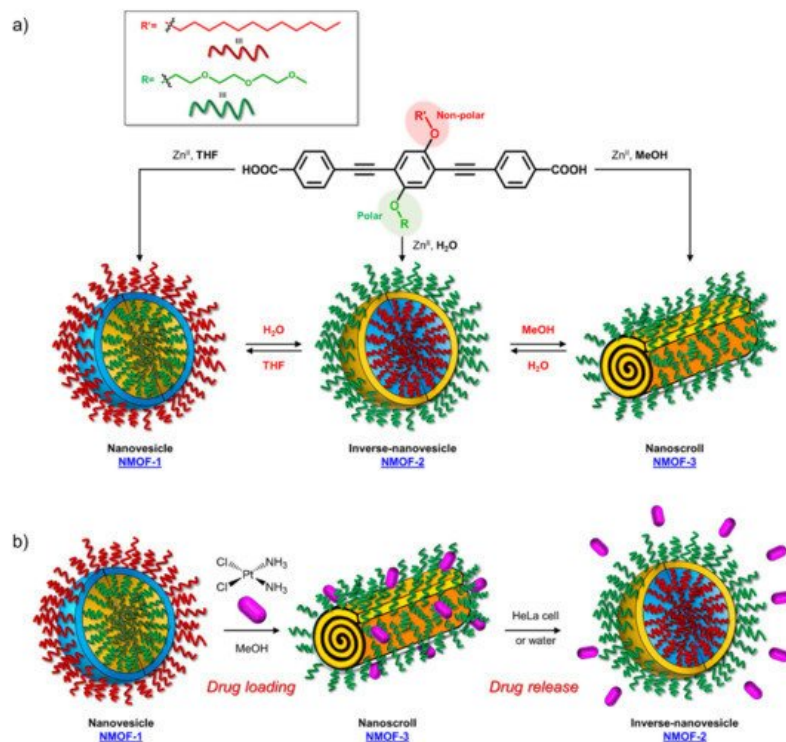


Figure 3. Schematic representation of (a) synthesis and morphology of NMOFs and (b) drug loading and release of cisplatin.

Another example of fluorescent-imaging molecules that are exploitable for medical application, such as photodynamic therapy (PDT), was reported by Barattucci et al. [12]. Photodynamic therapy is a very useful treatment in which the tumor tissues can be eradicated through the use of a photosensitizer which, after absorption of light, produces, in the presence of oxygen, highly reactive oxygen-based species (ROS) that damage the tumor cell, thereby inducing its death, by different modalities. The ideal photosensitizer should possess a low or absent dark toxicity, a high toxicity after light activation by a selective excitation wavelength, and chemical and physical stability but also a good facility in the distribution and elimination pathway. Encouraged by the good internalization in cells of the end-glucose amino OPEs **6** and **9** (Table 1), Barattucci et al. [11] tested the capability of these systems to work as photosensitizers and thus, based on the previous results, they synthesized 3-OPEs, which end with glucose units and with different functionalization on the aromatic rings for improving biocompatibility and solubility in aqueous media. After spectroscopic characterization, all compounds were tested for singlet oxygen production, through uric acid (UA) as the detector and methylene blue as the reference photosensitizer, thus recording the reduction of absorption of UA in the presence of the different OPEs. No singlet-oxygen production was recorded for the control OPE **5c**. The internalization of **6a** and **9a**, was conducted on HaCaT (immortalized human keratinocytes), HeLa, and Hep-2 cell lines. After the incubation of the two OPEs showed a good internalization, mainly in the Golgi apparatus and in the endoplasmic reticulum, an intense fluorescence allowed for imaging after the uptake, without any different behavior among the cell lines. In addition, none of the OPEs showed dark cytotoxicity at a concentration of 3 μ M, while a reduced cell viability (from 60% to 85 %) was found for higher concentrations, which are comparable to other commercial and approved drugs. The cytotoxicity, after UVA irradiation, was evaluated, and the findings highlighted its dependence from concentration and UVA dose, reaching the LD₅₀ dose with [OPE]= 3 μ M. Unfortunately, no selectivity among the tumor cell lines (HeLa and Hep-2) and nontumor line (HaCaT) was found. Studies on the cell morphology after PDT showed that only amino-OPEs cause a damage induced by ROS production in the microtubule network of the cancer cell, which in turn induces an alteration of the metaphase cell cycle. Therefore, these studies represent the first step to develop an OPE-based platform, which is made possible due to the photoluminescence features of OPEs for imaging as well as for PDT and medical applications.

3.2. OPEs as Sensors

Another important application of small luminescence molecules is represented by tracking or sensing. Different works have studied the use of OPEs for the detection of nitroaromatics (NACs) [52], as well as their use as a molecular junction for sensing hydrogen gas [53] or metal cations [54], and as a graphene oxide nanocomposite [55] for the recognition of dopamine and cysteine [56].

In this field, advances were obtained by Whitten's research group, who investigated the ability of OPEs to act as sensors for amyloids [20], whose existence is correlated to many neurodegenerative diseases, such as Parkinson's (PD) and Alzheimer's (AD) diseases. Common features for amyloid specific sensors are the presence of a linear conjugated and aromatic backbone, which promotes the binding to protein surface through hydrophobic interactions. PPEs were already used as probes for detection of protease [57] and phospholipase C [58] activity studies. In this study, OPEs with ethyl ester termini and of various charges and repeating units were studied as in vitro fluorescent probes for an amyloid model from hen egg white lysozyme (HEWL). Two groups of OPEs were analyzed, i.e., OPEs **18d-f** (Table 1) with positive alkyl ammonium pendants and different repeating units and an anionic OPE **19c**, which possesses sulfonated chain groups and a single repeating unit. The selected OPEs were achiral, amphiphilic, and water soluble, and as demonstrated previously [21], they enhanced their fluorescence when bounded to a hydrophobic surface because of a reduced water solvation quenching. All OPEs shown an increase in fluorescence intensity in the presence of amyloid and no fluorescence changes in presence of the monomeric form, except for OPE **19c**. The excitation spectra for all OPEs showed a bathochromic shift in the presence of amyloids and no change in the presence of a monomeric form. Furthermore, the induced circular dichroism (ICD) of an OPE–amyloid complex was analyzed in order to verify whether the intrinsic chirality of the proteins were transferred to the silent OPE chromophores when they are bonded into the complex form. No optical activities were recorded for cationic OPEs **18d-f** and **19c** with HEWL monomers; in the presence of HEWL amyloids, silent CD spectra were recorded for **18d**, whereas strong ICD signals were observed for **19c**, **18e**, and **18f**. Thus, according to the experimental results, the authors suggested that OPEs can bind to the proteins as single molecules or as J-dimers. In particular, for **18d** the spectroscopic evidence and the absence of optical activity suggest a noncooperative and saturable binding to the fibrils as single molecules rather than aggregates. Compound **19c** showed a nonspecific weak binding as J-dimers for monomeric proteins, probably due to hydrophobic and electrostatic interactions with the positive lysozyme (as already seen for similar PPEs [59]) and a stronger binding as J-dimers with fibril HEWL causing ICD signal. Finally, the spectroscopic evidence for longer cationic OPE **18e** and **18f** suggested a larger chiral J-aggregation on the amyloids surface (Figure 4). The interesting studies reported by Whitten described how OPEs can be used as selective sensing for amyloids fibril models, thereby exploiting their different spectroscopic behaviors (e.g., enhancement of fluorescence, induced circular dichroism) comparable to Thioflavin T (ThT), the most widely used dye for the detection of amyloids.

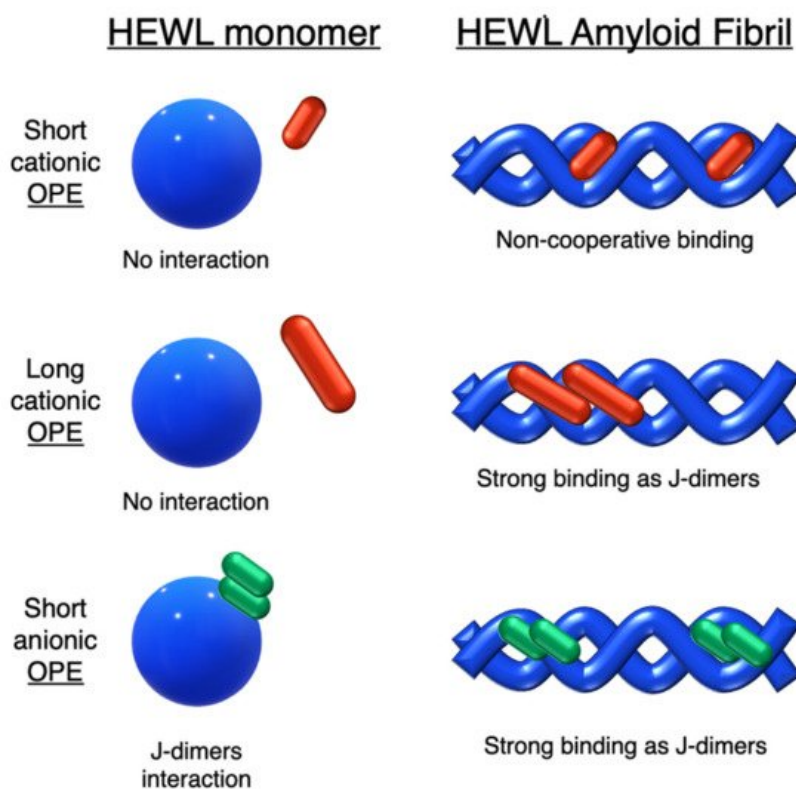


Figure 4. Schematic illustration of binding modes of OPEs **18d-f** (in red) and **19c** (in green) with HEWL and HEWL fibrils.

The same group in 2017 selected a small library of OPE and PPE derivatives [22] as amyloid trackers towards another amyloid protein model bovine insulin, which, in a fashion similar to the previously studied lysozyme [20], was able to form fibrils in acid and high temperature conditions. Unlike the lysozyme, bovine insulin shows a negatively charged surface at neutral pH. In order to verify the probe ability of these compounds, the excitation and emission fluorescence spectra of each compound were recorded both alone and after incubation with monomeric and fibril forms of HEWL and bovine insulin. Most of the studied compounds showed either a poor binding property toward the two proteins or no changes in

fluorescence after interaction and, consequently, the impossibility to use them as sensors. The oligomeric compounds with positive charges at the end of their backbones resulted in them not being usable for sensing. However, some oligomeric positive compounds have a good fibril selectivity, and some others present a monomeric selectivity. In particular, the cationic **18d** and the anionic **19c** (Table 1) can represent selective sensors for fibrils. Almost all active probe compounds showed a common terminal ethyl ester group, which guarantees, as demonstrated elsewhere [21], a fluorescence unquenching after interaction with hydrophobic molecules (such as amphiphiles or proteins), due to the removal of water molecules from a hydration shell. Among the positive ethyl ester terminated dyes, **18e** and **18f** showed an increased fluorescence intensity and thus a better selectivity for lysozyme fibrils over the monomeric form of HEWL. The opposite behavior was detected for insulin. In this case, a more intense fluorescence was recognized for the monomeric forms than fibrils, probably due to a coulombic interaction between the positive dyes **18e**, **18f**, and the negatively charged insulin monomer (Figure 5). Among the anionic OPEs, **19a** and **19b** exploited favorable coulombic interactions with the positive lysozyme surface, but the lack of ethyl ester terminal groups impeded the increasing of fluorescence after the binding event and thus prevents their use as sensors. The best candidate for amyloid sensing was **19c**: it showed an increase of fluorescence intensity in the presence of both lysozyme and insulin fibrils, although a very small fluorescence increase was observed for monomeric forms (Figure 5). This effect may be due to a higher solvation energy of the anionic **19c** with respect to the $-NMe_3^+$ functionalized OPEs. Furthermore, induced CD signals were recorded for **19c** with lysozyme and insulin fibrils, suggesting a chiral J-type dimer binding mode that was more pronounced for insulin. Finally, the probe size plays an important role: the polymeric molecules can largely self-aggregate, thus reducing their solubility and their emission intensity. The smaller OPEs are instead prone to form H-type aggregates with a loss of fluorescence yield. Among the **18d**, **18e**, and **18f**, which differ only in size, **18e** has the best performance; **18d** is too small and does not possess the requested hydrophobic surface to bind to the protein, while **18f** is not able to induce the shielding of water molecules in the ethyl ester terminal group and, because of its longer and rigid backbone, cannot fit well with the protein surface.

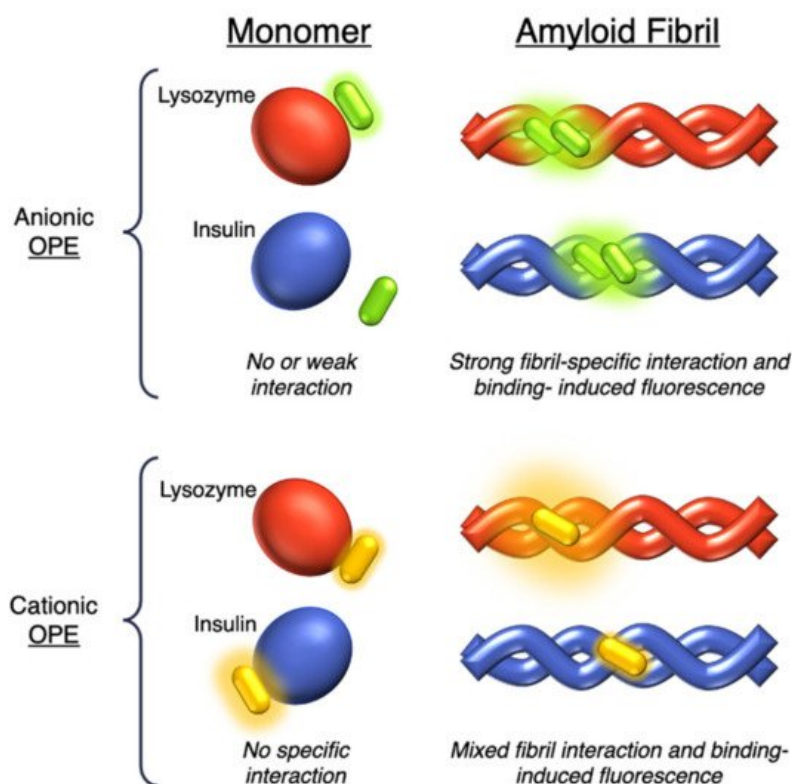


Figure 5. Schematic representation of the sensing modes of anionic **19c** (in green) and cationic **18d-f** (in yellow) OPEs towards lysozyme (in red) and insulin (in blue) monomers and fibrils.

Very recently, a remarkable improvement in this field was achieved by Chi et al., who used **19c** and **18e** (Table 1) for detecting fibrillar and prefibrillar amyloid proteins [23]. The two OPEs were tested as molecular sensors for fibrillar and prefibrillar aggregates of A β 40 and A β 42 peptides associated to AD and for four variants of α -synuclein (wild type and mutants A30P, E35K, and A53T) associated to PD over their monomeric counterparts. To evaluate the binding properties, the excitation and emission spectra of ThT (as a model compound), **19c**, and **18e** in the presence of monomeric and fibrillar A β 40 were measured. In buffer solution, OPEs showed low fluorescence intensities due to the water quenching effect, and no increase of fluorescence was recorded in the presence of the monomeric form of A β 40, except for a slight increase recorded for **18e**, probably attributable to the electrostatic interactions. On the other hand, a large fluorescence

amplification was produced when OPEs were mixed with A β 40 fibrils. This behavior was ascribed to the **18e** J-dimer formation by a stacking interaction, to the planarization of an aromatic backbone and the desolvation of ethyl ester terminal groups. Moreover, the ThT/fibril complex showed a fluorescence that is 10 to 30 times lower than the corresponding complexes with OPEs (Figure 6a). According to the spectroscopical results, all the analyzed compounds are selective for fibrils, but OPEs gave the best fluorescence response. Moreover, **18e** seemed to have a higher affinity toward longer fibrils obtained in tris buffer rather than toward the shorter ones in phosphate buffer, while **19c** exhibited a better affinity with shorter fibrils. For these reasons, supplementary binding studies were conducted with A β 42 and four α -synuclein forms. It was observed that A β 42 is the more amylogenic form of A β proteins, as its deposition starts prior to A β 40, showing even for unincubated A β 42 the presence of oligomeric and prefibrillar aggregates. The fluorescence spectra of ThT (20 μ M), **19c** (1 μ M), and **18e** (1 μ M) in the presence of either unincubated or incubated A β 42 (5 μ M) were recorded, showing for ThT and **19c** a small increase of the fluorescence intensity in the presence of an oligomeric form of A β 42 and a larger enhancement with the fibrillar form of the protein. On the contrary, **18e** showed a very intense fluorescence signal in the presence of both a prefibrillar and a fibrillar form. Thus, all compounds act as sensors for fibrils, but **18e** can act as a sensor also for a prefibrillar form in an early stage of amyloid formation. In fact, **18e** has shown different emission spectra with prefibrils and a larger fibrillar protein, indicating a different binding mode toward the two different targets. This result confirms the potentiality of **18e** to discriminate the two conformational forms of A β 42. In order to verify the ability of the OPEs to serve also as sensors for PA, which often correlated to AD pathology, the OPE spectroscopic responses were studied in the presence of α -synuclein fibrils. Oligomeric forms of α -synuclein were correlated to the disruption of mitochondrial activity, cellular membrane, and synapses. With this aim, the spectroscopic behaviors of OPEs toward an α -synuclein wild type and the three single mutant forms, A30P, A53T (involved in the early stage of PD), and E35K (which produces small oligomers), were analyzed. In particular, A30P aggregates more slowly than the wild type, while A53T seems to aggregate faster. ThT did not show significant changes in the excitation and emission, while on the contrary **19c** showed an increase of the intensities in the presence of all proteins except for A30P (probably due to a low abundance of oligomers) and was particularly intense for A53T. Compound **18e** in the presence of proteins showed similar behavior to **19c**, but the enhancement in this case was very pronounced (Figure 6b). All these results confirm the ability of the OPEs to act as sensors for prefibrillar and fibrillar aggregates that are already in the initial oligomeric form, thus representing a very powerful tool for the early diagnosis of AD and PD.

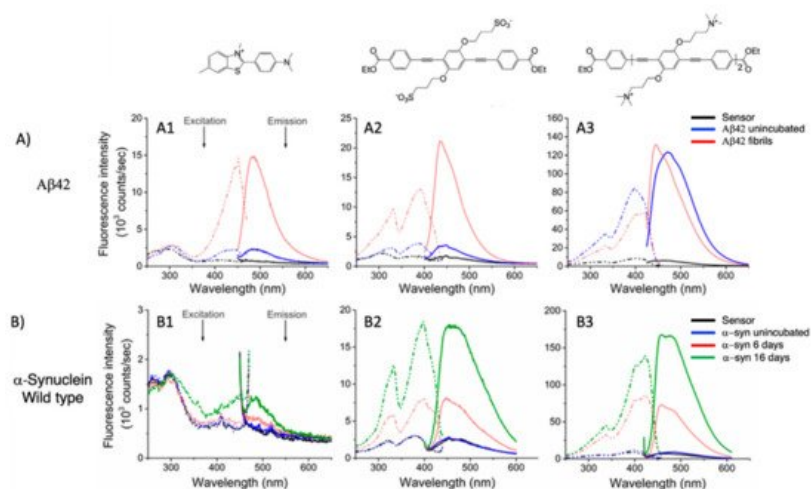


Figure 6. (A) Excitation (dashed line) and emission spectra (solid line) of ThT (A1), **19c** (A2), and **18e** (A3) in the presence of A β 42 (up) alone (black line), in the presence of A β 42 unincubated (blue line), and in the presence of A β 42 fibrils (red line). (B) Excitation (dashed line) and emission spectra (solid line) of ThT (B1), **19c** (B2), and **18e** (B3) in presence of α -synuclein wild type (bottom) alone (black line), in presence of α -synuclein unincubated (blue line), and in presence of α -synuclein after 6 days of incubation (red line) and after 16 days (green line). Adapted with permission from [23]. Copyright 2019 American Chemical Society.

Very recently, Evans et al. [24] carried out a computational investigation about the binding dynamics of compounds **19c** and **18e** (Table 1) toward some A β oligomer models using classical all-atom molecular dynamics, in order to understand their interaction with amyloids. The studies were conducted with two β -sheet rich A β oligopeptides of 5- and 24-mer. The simulations showed that both positive and anionic OPEs can bind to the 5-mer protein, with a smaller number of molecules for **18e** than **19c**. In particular, **18e** formed mainly dimers, while **19c** was bound to protein through tetramers or pentamers, probably because of the higher electrostatic repulsions present in the more charged **18e**. Furthermore, the small 5-mer oligopeptide possesses a small binding surface, which limits the possibility of larger OPEs to bind to it. On the other hand, a higher number of OPEs, as a single molecule, as well as aggregates, were able to bind with 24-mer oligopeptides, both in the outer surface and at the end portions. In analyzing the aminoacidic presence at the protein

surfaces, the kind and the charges of residue closer than 4 Å from OPE were determined. The binding sites for both OPEs presented mostly nonpolar residues (68% for **19c** and 77% for **18e**), while the ratio anionic/cationic residues was 0.25 for **19c** and 3 for **18e**, underlining the importance of a correct electrostatic interaction in the binding. In addition, in analyzing the reasons of the fluorescence enhancement of OPEs after the binding event, the authors found a planarization of the aromatic backbone, with an important reduction in the dihedral angle distribution (close to 0°) when OPEs were bound to protein as complex (trimers or more). These observations partially explain the fluorescence intensity enhancement. Furthermore, the enhancement of the fluorescence is in part attributed to the desolvation of the water molecules in the ester-end group. For this reason, the number of molecules of water around the end groups of OPEs was calculated with and without the 24-mer protein. For the free OPEs, there are 15 water molecules, while for a single-binding protein/**19c**, a reduction was observed with a further decrease when OPEs were bound to protein through tetramers or pentamers, confirming a binding-inducing unquenching process. Thus, the present study confirms and supports the previous experimental results, showing that OPEs, due to the balance of electrostatic interaction, the hydrophobicity of the backbone, and the right size, can represent good platforms for sensing fibrils and prefibrils in an early stage of disease.

Another interesting application of OPE derivatives as sensors for saccharides was proposed in 2011 by Zhao et al. [33]. In this case, two kinds of OPEs that were conjugated with linear **20** and cruciform **21** π -frameworks (Table 1) and functionalized with phenylboronic acid were used in physiological conditions for the detection of saccharides with high sensitivity. In the synthesized OPEs, the triazole linker was able to act as a hydrogen-bond donor to stabilize a boron-saccharide complex, as confirmed by NMR studies. Meanwhile, the OPE aromatic core guaranteed a fluorescence response to the boron-saccharide complex aggregation state in solution. In particular, the best results were obtained for the cruciform-like OPEs **21**; in the absence of sugar, the OPEs are prone to aggregate, while the binding to saccharides results in a decrease of the aggregate's dimensions, which in turn increases the fluorescence emission in a fluorescence turn-on sensing system.

References

1. Bunz, U.H.F. Poly(aryleneethynylene)s: Syntheses, Properties, Structures, and Applications. *Chem. Rev.* 2000, 100, 1605–1644.
2. Lakshmikantham, M.V.; Vartikar, J.; Jen, K.Y.; Cava, M.P.; Huang, W.S.; MacDiarmid, A.G. Poly(rho-phenylene xylydine): Synthesis and conductivity studies. *Am. Chem. Soc. Polym. Prepr. Div. Polym. Chem.* 1983, 24, 75.
3. Krywko-Cendrowska, A.; Szwed, D.; Szwed, R. Well-Defined Conjugated Macromolecules Based on Oligo (Arylene Ethynylene)s in Sensing. *Processes* 2020, 8, 539.
4. Schumm, J.S.; Pearson, D.L.; Tour, J.M. Iterative Divergent/Convergent Approach to Linear Conjugated Oligomers by Successive Doubling of the Molecular Length: A Rapid Route to a 128A-Long Potential Molecular Wire. *Angew. Chem. Int. Ed. Engl.* 1994, 33, 1360–1363.
5. Pertici, F.; Varga, N.; van Duijn, A.; Rey-Carrizo, M.; Bernardi, A.; Pieters, R.J. Efficient synthesis of phenylene-ethynylene rods and their use as rigid spacers in divalent inhibitors. *Beilstein J. Org. Chem.* 2013, 9, 215–222.
6. Wautelet, P.; Moroni, M.; Oswald, L.; Le Moigne, J.; Pham, A.; Bigot, J.-Y. Rigid Rod Conjugated Polymers for Nonlinear Optics. 2. Synthesis and Characterization of Phenylene-Ethynylene Oligomers. *Macromolecules* 1996, 29, 446–455.
7. Meza, D.; Arias, E.; Moggio, I.; Romero, J.; Mata, J.M.; Jiménez-Barrera, R.M.; Ziolo, R.F.; Rodríguez, O.; Ottonelli, M. Synthesis, Photophysical and Supramolecular Study of p-Conjugated (diethylene glycol methyl ether) Benzoateethynylene Oligomers and Polymer. *Polym. Chem.* 2015, 6, 1639–1648.
8. Castruita, G.; García, V.; Arias, E.; Moggio, I.; Ziolo, R.; Ponce, A.; González, V.; Haley, J.E.; Flikkema, J.L.; Cooper, T. Synthesis, optical and structural properties of sanidic liquid crystal (cholesteryl)benzoate-ethynylene oligomers and polymer. *J. Mater. Chem.* 2012, 22, 3770–3780.
9. García, M.C.; Turlakov, G.; Moggio, I.; Arias, E.; Valenzuela, J.H.; Hernández, M.; Rodríguez, G.; Ziolo, R.F. Synthesis and photophysical properties of conjugated (dodecyl)benzoateethynylene macromolecules: Staining of *Bacillus subtilis* and *Escherichia coli* rhizobacteria. *New J. Chem.* 2019, 43, 3332–3340.
10. Arias, E.; Méndez, M.T.; Arias, E.; Moggio, I.; Ledezma, A.; Romero, J.; Margheri, G.; Giorgetti, E. Supramolecular Recognition of *Escherichia coli* Bacteria by Fluorescent Oligo(Phenyleneethynylene)s with Mannopyranoside Termini Groups. *Sensors* 2017, 17, 1025.
11. Barattucci, A.; Deni, E.; Bonaccorsi, P.; Ceraolo, M.G.; Papalia, T.; Santoro, A.; Sciortino, M.T.; Puntoriero, F. Oligo(phenylene ethynylene) Glucosides: Modulation of Cellular Uptake Capacity Preserving Light ON. *J. Org. Chem.* 2014, 79, 5113–5120.

12. Deni, E.; Zamarron, A.; Bonaccorsi, P.; Carreño, M.C.; Juarranz, A.; Puntoriero, F.; Sciortino, M.T.; Ribagorda, M.; Barattucci, A. Glucose-functionalized amino-OPEs as biocompatible photosensitizers in PDT. *Eur. J. Med. Chem.* 2016, 111, 58–71.
13. Mancuso, A.; Barattucci, A.; Bonaccorsi, P.; Giannetto, A.; La Ganga, G.; Musarra-Pizzo, M.; Salerno, T.; Santoro, M.G. A.; Sciortino, M.T.; Puntoriero, F.; et al. Carbohydrates and Charges on Oligo(phenyleneethynyls): Towards the Design of Cancer Bullets. *Chem. Eur. J.* 2018, 24, 16972–16976.
14. Zhi, Y.G.; Lai, S.W.; Chan, Q.K.W.; Law, Y.C.; Tong, G.S.M.; Che, C.M. Systematic Studies on Photoluminescence of Oligo(arylene-ethynylene)s: Tunability of Excited States and Derivatization as Luminescent Labeling Probes for Proteins. *Eur. J. Org. Chem.* 2006, 2006, 3125–3139.
15. Yin, C.; Song, W.; Jiang, R.; Lu, X.; Hu, W.; Shen, Q.; Li, X.; Li, J.; Fan, Q.; Huang, W.; et al. Oligo(p-phenyleneethynylene) embedded amphiphiles: Synthesis, photophysical properties and self-assembled nanoparticles with high structural stability and photostability for cell imaging. *Polym. Chem.* 2014, 5, 5598–5608.
16. Hu, X.; Yin, C.; Hu, W.; Yang, Z.; Li, J.; Li, X.; Lu, X.; Zhao, H.; Tang, Y.; Fan, Q.; et al. Morphology-Tunable Fluorescent Nanoparticles: Synthesis, Photophysical Properties and Two-Photon Cell Imaging. *Chin. J. Chem.* 2015, 33, 888–896.
17. Yin, C.; Hong, B.; Gong, Z.; Zhao, H.; Hu, W.; Lu, X.; Li, J.; Li, X.; Yang, Z.; Fan, Q.; et al. Fluorescent oligo(p-phenyleneethynylene) contained amphiphiles-encapsulated magnetic nanoparticles for targeted magnetic resonance and two-photon optical imaging in vitro and in vivo. *Nanoscale* 2015, 7, 8907–8919.
18. Wang, J.; Zhou, L.; Sun, H.; Lv, F.; Liu, L.; Ma, Y.; Wang, S. Oligo(p-phenyleneethynylene) Derivatives for Mitochondria Targeting in Living Cells through Bioorthogonal Reactions. *Chem. Mater.* 2018, 30, 5544–5549.
19. Samanta, D.; Roy, S.; Sasmal, R.; Saha, D.N.; Pradeep, K.R.; Viswanatha, R.; Agasti, S.S.; Maji, T.K. Solvent adaptive dynamic metal-organic soft hybrid for imaging and biological delivery. *Angew. Chem.* 2019, 131, 5062–5066.
20. Donabedian, P.L.; Pham, T.K.; Whitten, D.G.; Chi, E.Y. Oligo(p-phenylene ethynylene) Electrolytes: A Novel Molecular Scaffold for Optical Tracking of Amyloids. *ACS Chem. Neurosci.* 2015, 6, 1526–1535.
21. Donabedian, P.L.; Creyer, M.N.; Monge, F.A.; Schanze, K.S.; Chi, E.Y.; Whitten, D.G. Controllable photosensitizer activity of OPEs. *Proc. Natl. Acad. Sci. USA* 2017, 114, 7278–7282.
22. Donabedian, P.L.; Evanoff, M.; Monge, F.A.; Whitten, D.G.; Chi, E.Y. Substituent, Charge, and Size Effects on the Fluorogenic Performance of Amyloid Ligands: A Small-Library Screening Study. *ACS Omega* 2017, 2, 3192–3200.
23. Fanni, A.M.; Monge, F.A.; Lin, C.-Y.; Thapa, A.; Bhaskar, K.; Whitten, D.G.; Chi, E.Y. High Selectivity and Sensitivity of Oligomeric p-Phenylene Ethynyls for Detecting Fibrillar and Prefibrillar Amyloid Protein Aggregates. *ACS Chem. Neurosci.* 2019, 10, 1813–1825.
24. Martin, T.D.; Brinkley, G.; Whitten, D.G.; Chi, E.Y.; Evans, D.G. Computational Investigation of the Binding Dynamics of Oligo p-Phenylene Ethynylene Fluorescence Sensors and Ab Oligomers. *ACS Chem. Neurosci.* 2020, 11, 3761–3771.
25. Wang, Y.; Schanze, K.S.; Chi, E.Y.; Whitten, D.G. When worlds collide interactions at the interface between biological systems and synthetic cationic conjugated polyelectrolytes and oligomers. *Langmuir* 2013, 29, 10635–10647.
26. Hill, E.H.; Stratton, K.; Whitten, D.G.; Evans, D.G. Molecular Dynamics Simulation Study of the Interaction of Cationic Biocides with Lipid Bilayers: Aggregation Effects and Bilayer Damage. *Langmuir* 2012, 28, 14849–14854.
27. Li, Y.; Guo, H. Atomistic simulations of an antimicrobial molecule interacting with a model bacterial membrane. *Theor. Chem. Acc.* 2013, 132, 1303–1311.
28. Scheberl, A.; Khalil, M.L.; Maghsoodi, F.; Strach, E.W.; Yang, J.; Chi, E.Y.; Schanze, K.S.; Reimhult, E.; Whitten, D.G. Quantitative Determination of Dark and Light-Activated Antimicrobial Activity of Poly(Phenylene Ethynylene), Polythiophene, and Oligo(Phenylene Ethynylene) Electrolytes. *ACS Appl. Mater. Interfaces* 2020, 12, 21322–21329.
29. Hill, E.H.; Evans, D.G.; Whitten, D.G. Photochemistry of “End-Only” Oligo-p-phenylene Ethynyls: Complexation with Sodium Dodecyl Sulfate Reduces Solvent Accessibility. *Langmuir* 2013, 29, 9712–9720.
30. Hill, E.H.; Pappas, H.C.; Evans, D.G.; Whitten, D.G. Cationic oligo-p-phenylene ethynyls form complexes with surfactants for long-term light-activated biocidal applications. *Photochem. Photobiol. Sci.* 2014, 13, 247–253.
31. Martin, T.D.; Hill, E.H.; Whitten, D.G.; Chi, E.Y.; Evans, D.G. Oligomeric Conjugated Polyelectrolytes Display Site-Preferential Binding to an MS2 Viral Capsid. *Langmuir* 2016, 32, 12542–12551.
32. Monge, F.A.; Jagadesan, P.; Bondu, V.; Donabedian, P.L.; Ista, L.; Chi, E.Y.; Schanze, K.S.; Whitten, D.G.; Kell, A.M. Highly Effective Inactivation of SARS-CoV-2 by Conjugated Polymers and Oligomers. *ACS Appl. Mater. Interfaces.* 2020, 12, 55688–55695.
33. Mulla, K.; Dongare, P.; Zhou, N.; Chen, G.; Thompson, D.W.; Zhao, Y. Highly sensitive detection of saccharides under physiological conditions with click synthesized boronic acid-oligomer fluorophores. *Org. Biomol. Chem.* 2011, 9, 1332–1

34. Gea, W.; Yub, Q.; López, G.P.; Stiff-Roberts, A.D. Antimicrobial oligo(p-phenylene-ethynylene) film deposited by resonant infrared matrix-assisted pulsed laser evaporation. *Colloids Surf. B Biointerfaces* 2014, 116, 786–792.
35. Yua, Q.; Geb, W.; Atewologun, A.; Stiff-Roberts, A.D.; López, G.P. Antimicrobial and bacteria-releasing multifunctional surfaces: Oligo (p-phenylene-ethynylene)/poly (N-isopropylacrylamide) films deposited by RIR-MAPLE. *Colloids Surf. B Biointerfaces* 2015, 126, 328–334.
36. Wang, Y.; Jones, E.M.; Tang, Y.; Ji, E.; Lopez, G.P.; Chi, E.Y.; Schanze, K.S.; Whitten, D.G. Effect of Polymer Chain Length on Membrane Perturbation Activity of Cationic Phenylene Ethynylene Oligomers and Polymers. *Langmuir* 2011, 27, 10770–10775.
37. Dascier, D.; Ji, E.; Parthasarathy, A.; Schanze, K.S.; Whitten, D.G. Efficacy of End-Only-Functionalized Oligo(arylene-ethynylene)s in Killing Bacterial Biofilms. *Langmuir* 2012, 28, 11286–11290.
38. Wang, Y.; Chi, E.Y.; Natvig, D.O.; Schanze, K.S.; Whitten, D.G. Antimicrobial Activity of Cationic Conjugated Polyelectrolytes and Oligomers against *Saccharomyces cerevisiae* Vegetative Cells and Ascospores. *ACS Appl. Mater. Interfaces* 2013, 5, 4555–4561.
39. Pappas, H.C.; Sylejmani, R.; Graus, M.S.; Donabedian, P.L.; Whitten, D.G.; Neumann, A.K. Antifungal properties of cationic phenylene ethynylenes and their impact on β -glucan exposure. *Antimicrob. Agents Chemother.* 2016, 60, 4519–4529.
40. Wang, Y.; Canady, T.D.; Zhou, Z.; Tang, Y.; Price, D.N.; Bear, D.G.; Chi, E.Y.; Schanze, K.S.; Whitten, D.G. Cationic Phenylene Ethynylene Polymers and Oligomers Exhibit Efficient Antiviral Activity. *ACS Appl. Mater. Interfaces* 2011, 3, 2209–2214.
41. Wang, J.; Zhuo, L.; Liao, W.I.; Yang, X.; Tang, Z.; Chen, Y.; Luo, S.; Zhou, Z. Assessing the Biocidal Activity and Investigating the Mechanism of Oligo-p-phenylene-ethynylenes. *ACS Appl. Mater. Interfaces.* 2017, 9, 7964–7971.
42. Liao, W.; Zhuo, L.-G.; Yang, X.; Zhao, P.; Kan, W.; Wang, G.; Song, H.; Wei, H.; Yang, Y.; Tian, G.; et al. Biocidal Activity and Mechanism Study of Unsymmetrical Oligo-Phenylene-Ethynylenes. *ACS Appl. Bio Mater.* 2020, 3, 5644–5651.
43. Yuan, Q.; Wang, Y.; Yao, P.; Lv, J.; Wang, Q.; Sun, F.; Feng, W. Effect of unsymmetrical oligo-phenylene-ethynylene OP E3 against multidrug-resistant bacteria in vitro and in vivo. *J. Chemother.* 2021, 33, 156–164.
44. Weerakkody, L.R.; Witharana, C. The role of bacterial toxins and spores in cancer therapy. *Life Sci.* 2019, 235, 116839.
45. Whitten, D.G.; Tang, Y.; Zhou, Z.; Yang, J.; Wang, Y.; Hill, E.H.; Pappas, H.C.; Donabedian, P.L.; Chi, E.Y. A Retrospective: 10 Years of Oligo(phenylene-ethynylene) Electrolytes: Demystifying Nanomaterials. *Langmuir* 2019, 35, 307–325.
46. Cardone, A.; Lopez, F.; Affortunato, F.; Busco, G.; Hofer, A.M.; Mallamaci, R.; Martinelli, C.; Colella, M.; Farinola, G.M. An arylenethynylene fluorophore for cell membrane staining. *Biochim. Biophys. Acta.* 2012, 1818, 2808–2817.
47. Terai, T.; Nagano, T. Fluorescent probes for bioimaging applications. *Curr. Opin. Chem. Biol.* 2008, 12, 515–521.
48. Tian, J.; Du, Y.; Tang, C.; An, Y. Fluorescence Molecular Imaging of Medicinal Chemistry in Cancer. *Top Med. Chem.* 2020, 34, 1–31.
49. Kim, T.; Jokers, J.V. Inorganic Fluorescent Nanomaterials. *Top Med. Chem.* 2020, 34, 55–80.
50. Cheng, H.-B.; Li, Y.; Tang, B.Z.; Yoon, J. Assembly strategies of organic-based imaging agents for fluorescence and photoacoustic bioimaging applications. *Chem. Soc. Rev.* 2020, 49, 21–31.
51. Yang, X.; Lovell, J.F.; Murthy, N.; Zhang, Y. Organic Fluorescent Probes for Diagnostics and Bio-Imaging. *Top Med. Chem.* 2020, 34, 33–53.
52. Wang, H.; He, G.; Chen, X.; Liu, T.; Dinga, L.; Fang, Y. Cholesterol modified OPE functionalized film: Fabrication, fluorescence behavior and sensing performance. *J. Mater. Chem.* 2012, 22, 7529–7536.
53. Xin, J.-G.; Yang, C.-L.; Wang, M.-S.; Ma, X.-G. OPE molecular junction as a hydrogen gas sensor. *Curr. Appl. Phys.* 2018, 18, 273–279.
54. Yan, F.; Chen, F.; Wu, X.-H.; Luo, J.; Zhou, X.-S.; Horsley, J.R.; Abell, A.D.; Yu, J.; Jin, S.; Mao, B.-W. Unique Metal Cation Recognition via Crown Ether-Derivatized Oligo(phenyleneethynylene) Molecular Junction. *J. Phys. Chem. C.* 2020, 124, 8496–8503.
55. Deng, J.; Liu, M.; Lin, F.; Zhang, Y.; Liu, Y.; Yao, S. Self-assembled oligo(phenylene ethynylene)s/graphene nanocomposite with improved electrochemical. *Anal. Chim. Acta.* 2013, 767, 59–65.
56. Adachi, N.; Yoshinari, M.; Suzuki, E.; Okada, M. Oligo(p-phenylene ethynylene) with Cyanoacrylate Terminal Groups and Graphene Composite as Fluorescent Chemical Sensor for Cysteine. *J. Fluoresc.* 2017, 27, 1449–1456.

57. Pinto, M.R.; Schanze, K.S. Amplified fluorescence sensing of protease activity with conjugated polyelectrolytes. *Proc. Natl. Acad. Sci. USA* 2004, 101, 7505–7510.
 58. Liu, Y.; Ogawa, K.; Schanze, K.S. Conjugated Polyelectrolyte Based Real-Time Fluorescence Assay for Phospholipase C. *Anal. Chem.* 2008, 80, 150–158.
 59. Kim, I.-B.; Dunkhorst, A.; Bunz, U.H.F. Nonspecific Interactions of a Carboxylate-Substituted PPE with Proteins. A Cautionary Tale for Biosensor Applications. *Langmuir* 2005, 21, 7985–7989.
-

Retrieved from <https://encyclopedia.pub/entry/history/show/25212>